Original Article

Utility of cytokeratin 7, S100A1 and caveolin-1 as immunohistochemical biomarkers to differentiate chromophobe renal cell carcinoma from renal oncocytoma

Keng Lim Ng[1,2,3], Robert J. Ellis[2,3], Hemamali Samaratunga[4], Christudas Morais[2,3], Glenda C. Gobe[3,5,6], Simon T. Wood[2,3]

[1]Department of Urology, Frimley Park Hospital, Frimley, UK; [2]Department of Urology, Princess Alexandra Hospital, Brisbane, Australia; [3]Centre for Kidney Disease and Research, Faculty of Medicine, University of Queensland, Brisbane, Australia; [4]Aquesta Pathology, Toowong, Australia; [5]School of Biomedical Sciences, [6]NHMRC Centre for Research Excellence CKD.QLD, Faculty of Medicine, University of Queensland, Brisbane, Australia

Contributions: (I) Conception and design: KL Ng, H Samaratunga, C Morais, GC Gobe, ST Wood; (II) Administrative support: All authors; (III) Provision of study materials or patients: KL Ng, H Samaratunga; (IV) Collection and assembly of data: All authors; (V) Data analysis and interpretation: All authors; (VI) Manuscript writing: All authors; (VII) Final approval of manuscript: All authors.

Correspondence to: Keng Lim Ng. Department of Urology, Frimley Park Hospital, Portsmouth Rd, Frimley, GU16 7UJ, UK. Email: keng.ng@nhs.net.

Background: Differentiation of chromophobe renal cell carcinoma (chRCC) from benign renal oncocytoma (RO) can be challenging especially when there are overlapping histological and morphological features. In this study we have investigated immunohistochemical biomarkers (cytokeratin 7/CK7, Caveolin-1/Cav-1 and S100 calcium-binding protein A1/S100A1) to aid in this difficult differentiation and attempted to validate their use in human renal tumour tissue to assess their discriminatory ability, particularly for chRCC and RO, in an Australian cohort of patients.

Methods: Retrospective study was carried out of archived formalin-fixed paraffin-embedded renal tumours from tumour nephrectomy specimens of 75 patients: 30 chRCC, 15 RO and 30 clear cell RCC (ccRCC). Sections were cut and immunostained with specific polyclonal antibodies of CK7, Cav-1 and S100A1. Morphometry was used to determine expression patterns of the biomarkers using Aperio ImageScope. Results were assessed with student *t*-test and ANOVA with significance at $P<0.05$.

Results: From this cohort, male-to-female ratio was 1.9:1. Median age was 64 (45–88 years) and median tumour size was 3.8 cm (range, 1.2–18 cm). There were 47 (62.7%) T1, 7 T2, 20 T3 and one T4 stage of RCC; with 2 patients presenting with M1 stage. There was significantly higher CK7 expression in chRCC compared to RO ($P=0.03$), and chRCC also had a different staining pattern and higher expression of Cav-1 compared to RO. There was higher expression of S100A1 in RO compared to chRCC.

Conclusions: Immunohistochemical staining and standard morphometry of CK7, Cav-1 and S100A1 can aid in the differentiation of chRCC and RO. This may guide clinicians in management of patients when faced with difficult diagnostic histological distinction between the two tumour subtypes.

Keywords: Renal cell carcinoma (RCC); chromophobe; oncocytoma; immunohistochemistry; cytokeratin 7; caveolin-1; S100A1

Submitted Oct 12, 2018. Accepted for publication Nov 12, 2018.
doi: 10.21037/tau.2018.11.02
View this article at: http://dx.doi.org/10.21037/tau.2018.11.02

Introduction

In the last decade, the incidence of renal tumours has risen substantially (1). Despite advances in radiological imaging and improved techniques of renal lesion biopsy, accurate diagnosis often eludes clinicians and final pathological diagnoses are only made postoperatively. A significant proportion of these renal lesions are benign, thus subjecting patients to unnecessary surgery and significant nephron loss (1). The most common malignant renal lesion is renal cell carcinoma (RCC). Within RCC, the most common histological subtypes of RCC are clear cell RCC (ccRCC) at approximately 75%, papillary RCC at 10%, chromophobe RCC (chRCC) at 5%, cystic solid RCC at 1–4% and collecting duct RCC at 1%. Accurate molecular biomarkers which can accurately distinguish RCC subtypes, and benign from malignant renal tumours, can potentially reduce unnecessary surgery, preserve nephron mass, and subsequently reduce development of chronic renal insufficiency associated with nephrectomy.

While ccRCC has morphological and histological characteristics that make its diagnosis relatively routine, one significant problem presented to pathologists is the distinction of malignant chRCC from benign renal oncocytoma (RO), as histological, morphological and histochemical features often overlap between these two entities. Accurate diagnosis of the pathological specimens is crucial as this dictates further surveillance and potential management for malignant chRCC compared with benign RO cases, where active surveillance may be adequate. Therefore novel and reproducible biomarkers which can effectively aid in the differential diagnoses of chRCC from RO are needed. Further characterisation of molecular signatures for renal tumour subtypes will help solve some of the diagnostic issues mentioned above. This may in turn lead to improved treatment algorithms with reduction of overtreatment of benign/indolent renal lesions leading to efficient management of healthcare costs. Previous studies have investigated the roles of various immunohistochemical biomarkers in this respect (2). The use of a panel of immunohistochemical biomarkers may be beneficial.

In this study, we evaluate expression patterns of cytokeratin-7 (CK7), Caveolin-1 (Cav-1) and S100 calcium-binding protein A1 (S100A1) in an Australian cohort of patients with renal tumours. CK7 is a low molecular weight keratin, belonging to a large family of structural polypeptides that are the fundamental markers of epithelial differentiation. The CKs found in simple epithelia (CK7, CK8, CK18 and CK19) are widely expressed in non-neoplastic kidney and renal neoplasms (3). Cav-1 is a 24 kDa membrane protein present in most cells and is a major component of membrane caveolae. Functionally, Cav-1 serves important roles in macromolecular transcytosis, endocytosis of pathogens, lipid metabolism and cellular signal transduction (4). S100A1 is a member of the S100 family of calcium binding molecules, most of which are clustered on chromosome 1q21, and are expressed in RCC (5). Importantly, these proteins are all involved in cell cycle progression and cell differentiation (6), and therefore implicated in tumorigenesis, a basis for their investigation in renal tumour subtypes.

Methods

Immunohistochemistry

Retrospective study was carried out of archived formalin-fixed paraffin-embedded renal tumours from tumour nephrectomy specimens of 75 patients for whom clinical characteristics were also available: 30 chRCC, 15 RO and 30 clear cell RCC (ccRCC). Each of the sections had some non-cancerous kidney as well as the tumour. This was assessed as "non-neoplastic" or "non-cancer" kidney tissue. Paraffin blocks of archived human renal tumour tissue were obtained from Aquesta Pathology (Toowong, Australia). The archived tissue blocks were collected retrospectively from a period 2009–2014. The ethics approval for scientific use of archived pathology samples was obtained from the Aquesta Pathology Ethics Committee (protocol 14/02). The immunohistochemistry methods are detailed below. Antibody optimisation and positive control tissue samples (tissue microarray of human liver, kidney and gut) were used to verify the staining activity of the biomarker in human tissue. Negative controls without primary antibody were prepared for each batch stain.

S100A1 was manually batch-stained for immunohistochemistry. Sections were dewaxed in xylene and rehydrated through descending graded alcohols to water using standard protocol. The sections were then transferred to Tris buffered saline (TBS) pH 7.6. Endogenous peroxidase activity in sections was blocked using 2.0% hydrogen peroxide (H_2O_2) in TBS for ten minutes. Sections were then washed in three changes of water, and transferred into buffer and subjected to 15 minutes antigen retrieval at 105 °C using a Biocare Medical decloaking chamber. On completion of the cooling cycle, the slides were allowed to cool for 20 minutes on the bench before transferring

back to TBS. They were washed in 3 changes of TBS then nonspecific antibody or peroxidase binding was inhibited by incubating the sections in Biocare Medical Background Sniper for 15 minutes. In a humidified chamber excess Sniper was decanted from the sections and the primary antibody. Sigma purified rabbit anti-S100A1 (1:125 dilution) (HPA006462) was applied for 60–90 minutes at room temperature. Sections were washed in three changes of TBS. A detection kit of specific secondary antibodies (MACH 2 Rabbit HRP secondary Ab; Biocare Medical, USA) was applied for 30 minutes. Sections were washed in three changes of TBS, then signals were developed in the chromogen betazoid diaminobenzidine hydrochloride (DAB) (MACH1 kit) for 5 minutes. Sections were washed in water three times to remove excess chromogen, then lightly counterstained in haematoxylin, washed in water, dehydrated through ascending graded alcohols, cleared in xylene, and mounted using DePex.

The immunohistochemistry for CK7 and Cav-1 was performed with an automatic Ventana Discovery ULTRA Stainer (Ventana Medical Systems Inc, Roche) using set protocols. The slides were placed into the Ventana automated stainer with primary CK7 (Santa Cruz mouse anti-CK7; 1:75 dilution); Cav-1 (Santa Cruz rabbit anti-Cav-1 sc-894; 1:250 dilution) and secondary antibodies (for CK7, Anti-mouse HQ; for Cav-1, MACH2 HRP anti-rabbit polymer) added to the autostainer at specific stages. Following staining, the slides were then dehydrated and cleared in xylene before coverslips were mounted automatically.

Morphometry analysis

Based on the staining characteristics of the immunohistochemical biomarkers, overall, nuclear and membrane expression was analysed on Aperio ImageScope (Leica Biosystems, Germany). Stained slides were scanned with an Aperio ScanScope XT slide scanning system (Aperio Technologies, USA) at 20× Aperio magnification. Digital images of the sections were captured using Aperio ImageScope software. A quantitative scoring of expression intensity and localisation of the various immunohistochemical biomarkers was analysed with respect to overall, nuclear and membrane expression.

Overall positive pixel expression analysis

Three random fields of the same size were selected for each RCC and paired non-neoplastic kidney section, using DAB as the positive chromogen. Analysis was carried out using the Positive Pixel Count v9 algorithm (for total staining intensity) from the Aperio ImageScope software. Staining (% positive pixels) was scored according to the intensity and percentage of cells stained. The intensity output for the Positive Pixel Count v9 algorithm was given as number of negative, weak positive, positive or strong positive pixels. Overall positive pixel count (%) was calculated by adding the values for "positive %" and "strong positive %" pixels.

The average of the three overall positive pixels % from the three respective scanned fields of renal tumour sections was obtained. Similarly, the average overall % positive pixels for three random fields in the non-neoplastic kidney sections, paired to a particular tumour, was obtained. Subsequently, the intensities of tumour and non-neoplastic kidney values were normalised against respective non-neoplastic kidney regions and the data were expressed as the percentage of overall non-neoplastic values.

Nuclear expression analysis

Three random fields of the same size were selected for each RCC and paired non-neoplastic kidney section. Analysis was carried out using the algorithm IHC Nuclear v1.0 from the Aperio ImageScope software. The output for IHC Nuclear v1 algorithm was given as a percentage of pixels with 0, 1+, 2+ or 3+ staining intensity. Nuclear positive pixels (%) were calculated by adding the values for 2+ % and 3+ % staining. The average of the three nuclear positive pixels from three non-neoplastic sections and average of three nuclear positive pixels from three tumour regions were then calculated. These were then made into average nuclear percentage. The nuclear intensities of tumour and non-neoplastic kidney were normalised against respective non-neoplastic regions and the data were expressed as the percentage of non-neoplastic values.

Membrane expression analysis

Three random fields of the same size were selected for each RCC and paired non-neoplastic kidney section. Analysis was carried out using algorithm IHC Membrane v1.0 from the Aperio ImageScope software. The output for IHC Membrane v1 algorithm was given as percentage of pixels with 0, 1+, 2+ or 3+ staining intensity. Membrane positive pixels (%) were calculated by adding the values for 2+ % and 3+ % staining. The average of the three membrane positive

Table 1 Clinicopathological characteristics of the cohort of RCC patients

Patients	75
Period	2009–2014
Gender	49 male; 26 female
Median age (years)	64 [18–88]
Median size (cm)	3.8 (1.2–18)
Subtype	30 ccRCC
	30 chRCC
	15 RO
T1 stage	47 (62.7)
T2 stage	7 (9.3)
T3 stage	20 (26.7)
T4 stage	1 (1.3)
M1 stage	2 (2.7)
Fuhrman (ccRCC)	
Grade 2	63.3%
Grade 3	20%
Grade 4	16.7%

pixels from three non-neoplastic sections and average of three membrane positive pixels from three tumour regions was then calculated. These were then made into average membrane percentage. The membrane intensities were normalised against respective non-neoplastic regions and the data were expressed as the percentage of normal values.

All the intensity results (overall, nuclear and membrane) were calculated using Excel. The results of non-neoplastic kidney (overall, nuclear and membrane) % change and tumour (overall, nuclear and membrane) % change were then tabulated and analysed with Graphpad Prism 6 (GraphPad Software, Inc). Graphs were generated to show the % expression change for tumour versus non-neoplastic kidney. Results were assessed with Student *t*-test and ANOVA with significance at P<0.05.

Results

Clinical characteristics of RCC nephrectomy patients

Ratio of males-to-females was 1.9:1, with the median age of 64 years (range, 18–88 years), in concordance with more RCC in males than females, and most patients being in the 50–70 age group. The median renal tumour size from this series was 3.8 cm (range, 1.2–18.0 cm). Thirty ccRCC, 30 chRCC and 15 RO were investigated. Although the ultimate aim was identifying immunohistochemical biomarkers that differentiated chRCC and RO, ccRCC were included for completeness as this subtype of RCC is the most common. The low number (15 cases) of RO was because RO account for approximately only 5% of all adult renal tumours (7). Among the ccRCC cases, 63.3% were Fuhrman grade 2, 20% grade 3 and 16.7% grade 4. The histopathological diagnoses were made by an experienced uropathologist. Although it is recognised that the system for grading RCC has been modified over the past two years (8), these samples were graded using the older Fuhrman grading system, and these grades are therefore reported for these specimens.

One third of the patients underwent partial nephrectomy (25 out of 75 patients). The majority of the patients were in stage T1 (62.7%), and the rest were T2 (9.3%), T3 (26.7%) and T4 (1.3%). The trend of patients presenting with smaller confined tumours in T1 stage is due to increasing detection rates for incidental renal tumours from widespread availability of radiological imaging, as also reported by other published series (9). There were only two patients with metastatic disease, and these patients underwent cytoreductive nephrectomy. These results are summarised in *Table 1*.

Immunohistochemistry of CK7

In the present study, non-cancer kidney cortical tissue adjacent to the tumours showed positivity for CK7 in the cytoplasm of distal tubular cells. There was strong membranous and cytoplasmic expression of CK7 in chRCC, with minimal or no staining in ccRCC and RO, as seen in *Figure 1*. In chRCC, there was intense cytoplasmic immunostaining with characteristic strong peripheral membrane staining. Based on the immunohistochemical characteristics, overall positive pixel expression was analysed using Aperio ImageScope.

Morphometry and overall expression of CK7

The overall positive pixel expression in tumour (ccRCC, chRCC and RO included) was lower compared to non-neoplastic kidney tissue (*Figure 2*). When compared separately, ccRCC and RO had significantly lower overall positive pixel expression compared to non-neoplastic tissue (P<0.0001 and P=0.002 respectively) (*Figure 2B,D*).

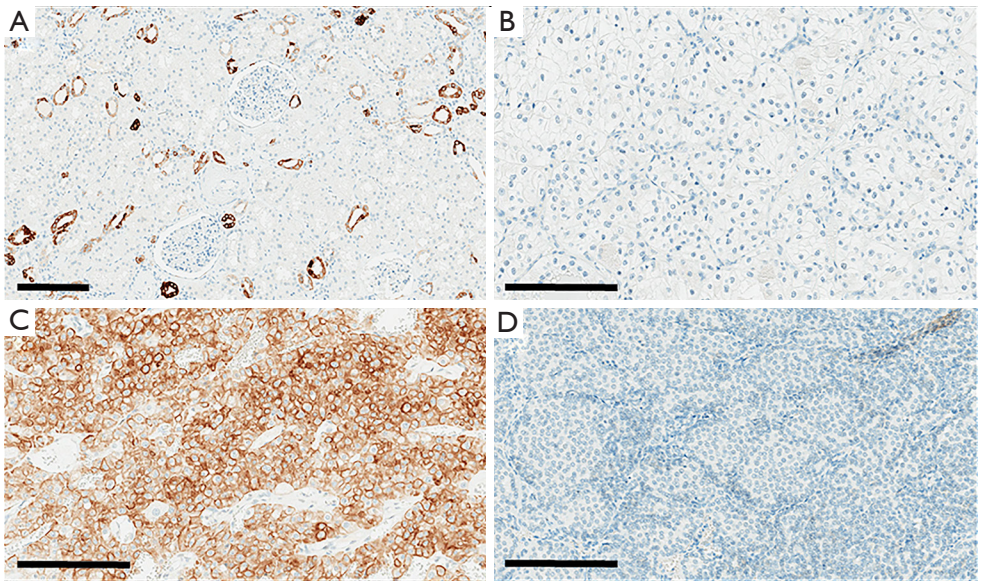

Figure 1 CK7 immunohistochemistry. (A) Immunostaining in non-neoplastic renal cortical tissue shows CK7 positivity in the vessels and some tubular epithelium; (B) in clear cell renal cell carcinoma (RCC), minimal CK7 expression is visible; (C) CK7 expression is strong in chromophobe RCC; (D) renal oncocytoma was clear of CK7 staining. Scale bar =200 µm.

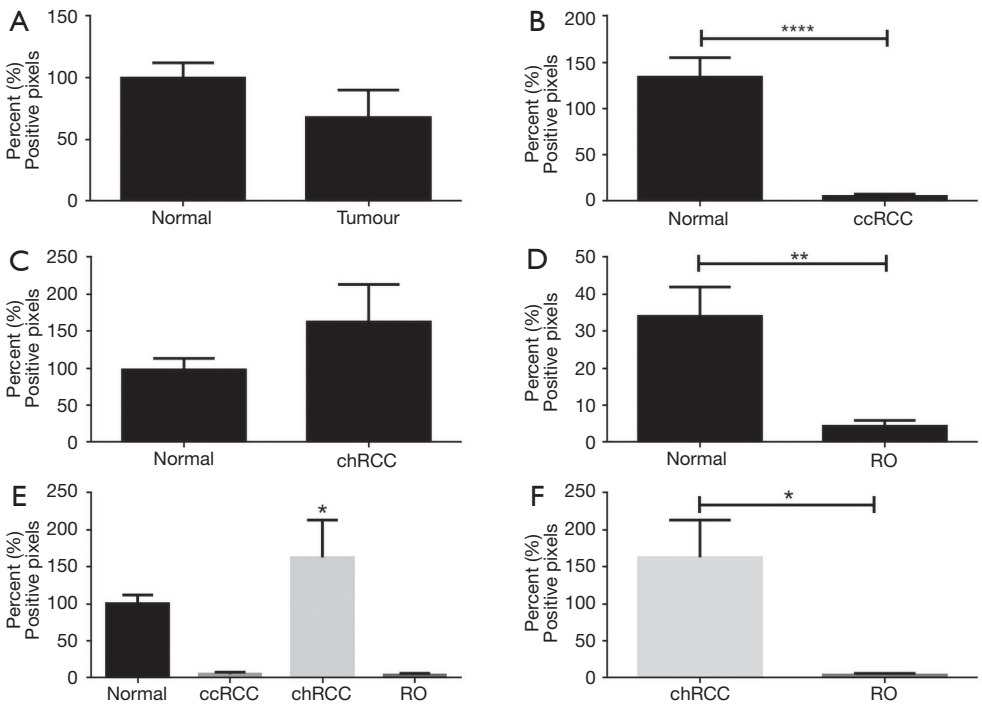

Figure 2 Expression of CK7 in renal tumours and matched non-neoplastic renal tissue. (A) Expression of CK7 in non-neoplastic *vs.* tumour tissue; (B) decreased expression of CK7 in clear cell (cc) renal cell carcinoma (RCC) *vs.* non-neoplastic kidney tissue (****, P<0.001); (C) expression of CK7 in chromophobe (ch) RCC *vs.* non-neoplastic kidney was increased, but differences did not reach conventional levels of statistical significance; (D) decreased expression of CK7 in renal oncocytoma (RO) *vs.* non-neoplastic kidney (**, P=0.002); (E) expression of CK7 across all tumour subtypes. Expression of CK7 in chromophobe chRCC was significantly higher compared with RO (*, P=0.03) and ccRCC (P=0.003); (F) significantly increased expression of CK7 was seen in chRCC *vs.* RO (*, P=0.03).

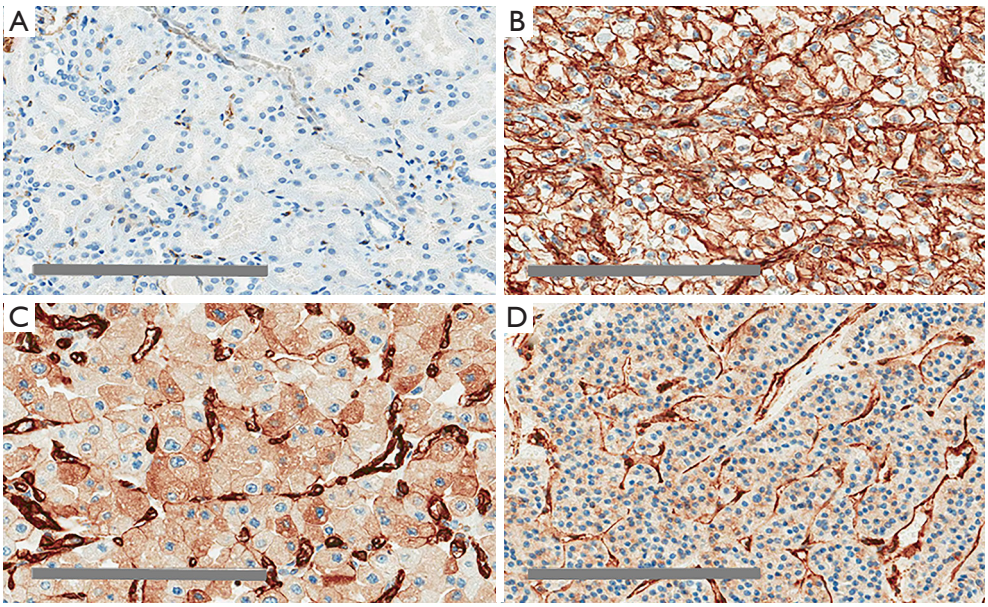

Figure 3 Caveolin-1 immunohistochemistry. (A) Immunostaining of Cav-1 in non-neoplastic renal cortical tissue localised to cytoplasm of the cells of the distal convoluted tubule and vascular endothelial cells. Proximal tubular epithelial cells were clear of Cav-1; (B) in clear cell renal cell carcinoma (RCC), Cav-1 staining was mainly membranous; (C) strong diffuse Cav-1 cytoplasmic staining with peripheral enhancement and a perinuclear halo was noted in chromophobe RCC; (D) patchy granular cytoplasmic staining was seen in renal oncocytoma. Scale bar =200 µm.

However, overall expression of CK7 was higher in chRCC compared to non-neoplastic kidney tissue (*Figure 2C*). Therefore, the expression of CK7 immunostaining was higher in chRCC when compared to RO and ccRCC (*Figure 2E*). Importantly, there was significantly higher expression of CK7 in chRCC compared with RO (P=0.03) as shown in *Figure 2F*. This significantly different expression pattern of CK7 in both chRCC and RO provides a useful and efficient immunohistochemical biomarker that can aid in differentiating the two entities.

Immunohistochemistry of Cav-1

In non-neoplastic kidney tissue, there was minimal basolateral membrane and cytoplasmic staining in distal convoluted tubules, along with staining of vascular endothelial cells. The immunostaining patterns of Cav-1 were mainly membranous in ccRCC, diffuse cytoplasmic in chRCC and patchy cytoplasmic in RO, as shown in *Figure 3A,B,C,D*. On closer inspection, there was a distinguishing staining pattern observed in chRCC where there was diffuse cytoplasmic staining with peripheral membranous enhancement and a perinuclear halo; compared to patchy granular cytoplasmic staining in RO (*Figure 3C,D*). This distinctly different Cav-1 immunostaining pattern between chRCC and RO may prove to be useful in separating the two tumour subtypes. Based on the immunohistochemical staining patterns, overall and membrane expressions were analysed on Aperio ImageScope.

Morphometry and overall expression of Cav-1

All tumours (including ccRCC, chRCC and RO) had significantly higher overall expression (P<0.0001) of Cav-1 compared with non-neoplastic kidney cortical tissue (*Figure 4A*). Individually, ccRCC Cav-1 expression was significantly higher compared with non-neoplastic kidney (P=0.01, *Figure 4B*), as was the case for chRCC (P<0.0001, *Figure 4C*), and RO (P=0.003, *Figure 4D*). There was no significant difference in Cav-1 expression between different neoplasms (*Figure 4E*). In particular, there was no significant difference in overall Cav-1 expression in chRCC versus RO. Notwithstanding, as shown in *Figure 3*, there may be useful discriminatory features in the different staining patterns between chRCC and RO.

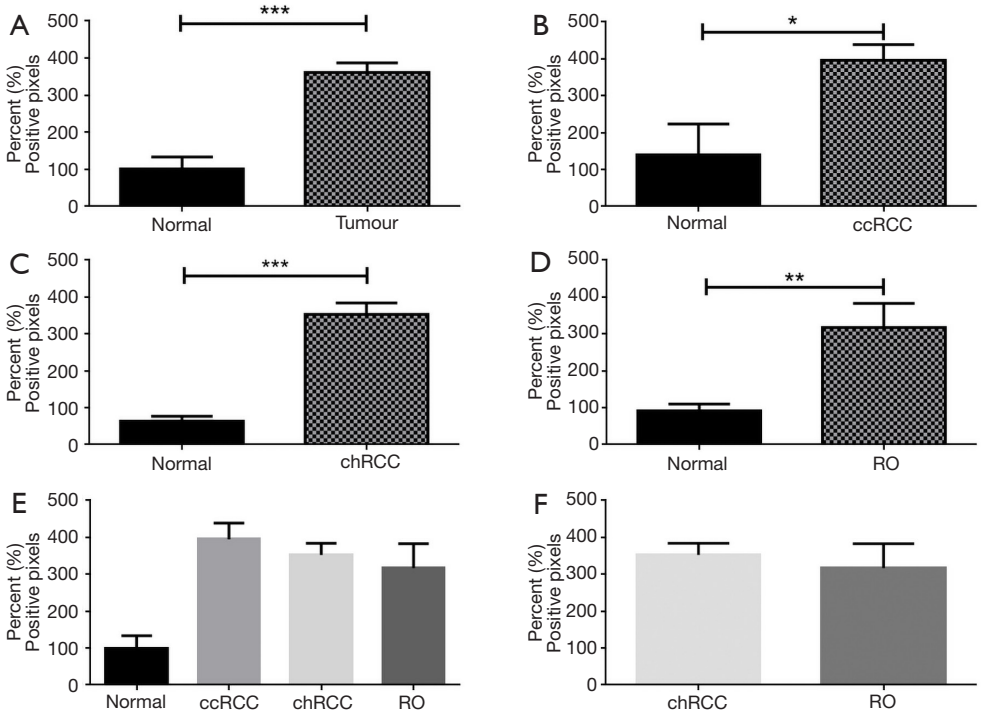

Figure 4 Expression of Cav-1 in renal tumours and matched non-neoplastic renal tissue. (A) Increased expression of Cav-1 in tumour *vs.* non-neoplastic tissue (***, P<0.0001); (B) increased overall Cav-1 expression in clear cell (cc) renal cell carcinoma (RCC) *vs.* non-neoplastic kidney (*, P=0.01); (C) increased overall Cav-1 expression of chromophobe (ch) RCC *vs.* non-neoplastic kidney (***, P<0.0001); (D) increased overall Cav-1 expression in renal oncocytoma (RO) *vs.* non-neoplastic kidney (**, P=0.003); (E) expression of Cav-1 across tumour subtypes; (F) overall expression of Cav-1 in chRCC *vs.* RO.

Cav-1 membrane expression

Since there was notable membranous enhancement in ccRCC and chRCC, the membranous immunostaining of Cav-1 was analysed quantitatively using Aperio ImageScope. Membranous expression of all tumours (ccRCC, chRCC, and RO) was significantly higher when compared to non-neoplastic kidney tissue (P<0.0001; *Figure 5A*). When individual subtypes were compared with non-cancer tissue, ccRCC, chRCC and RO differed significantly from non-cancer kidney (P<0.0001, P<0.0001 and P=0.003 respectively; *Figure 5B,C,D*). Membranous expression in ccRCC, chRCC and RO did not differ significantly (*Figure 5E*). Despite a higher membranous Cav-1 expression in chRCC compared to RO, this difference did not reach statistical significance (P=0.10; *Figure 5F*).

Immunohistochemistry of S100A1

S100A1 stained the cytoplasm of proximal and distal tubular cells in non-neoplastic kidney tissue. In ccRCC, there was both cytoplasmic and membranous immunostaining noted. There was patchy cytoplasmic staining noted in chRCC while in RO, there was intense and diffuse cytoplasmic and nuclear staining (*Figure 6A,B,C,D*). Overall and nuclear expression was analysed on Aperio ImageScope based on the immunohistochemical staining patterns of S100A1.

Overall expression patterns of S100A1

All tumours recorded a higher expression of S100A1 compared to non-neoplastic kidney as shown in *Figure* 7, but this did not reach significance. That trend persisted for ccRCC and chRCC, but in RO, there was significantly higher expression of S100A1 compared to non-neoplastic kidney (P=0.02) (*Figures* 7*B,D*). There was no significant difference in expression between RO and chRCC (*Figure* 7*E,F*).

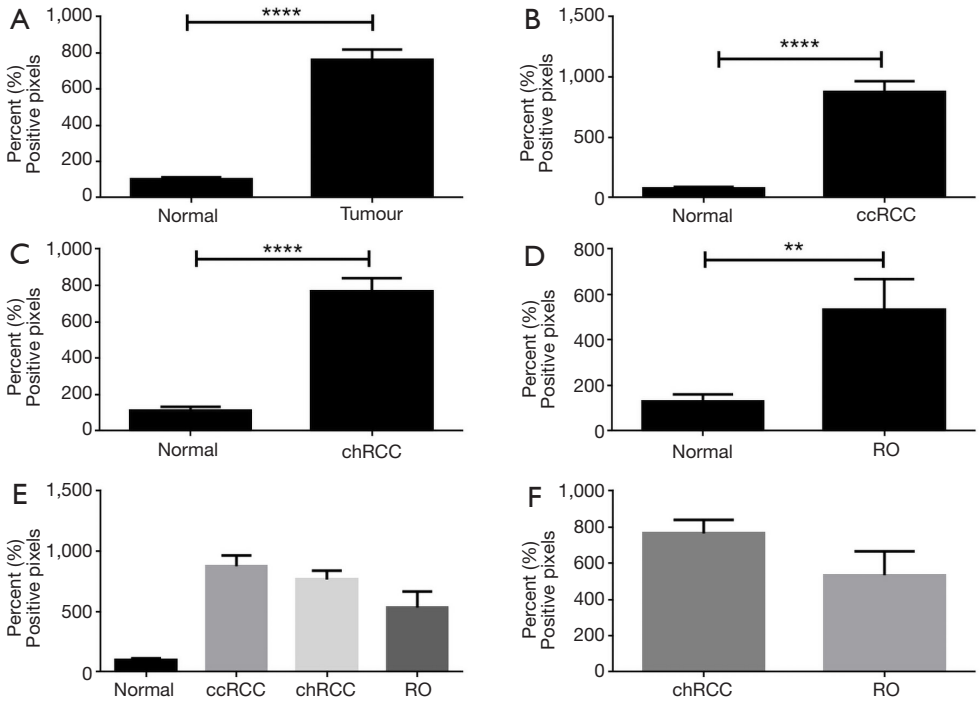

Figure 5 Expression of Cav-1 (membranous) in tumours and matched non-neoplastic renal tissue. (A) increased membranous expression of Cav-1 in tumour *vs.* non-neoplastic kidney (****, P<0.0001); (B) increased membranous Cav-1 expression in clear cell (cc) renal cell carcinoma (RCC) *vs.* non-neoplastic kidney (****, P<0.0001); (C) increased membranous Cav-1 expression of chromophobe (ch) RCC *vs.* non-neoplastic kidney (P<0.0001); (D) increased membranous Cav-1 expression in renal oncocytoma (RO) *vs.* non-neoplastic kidney (**, P=0.003); (E) expression of Cav-1 (membranous) across tumour subtypes; (F) expression of Cav-1 (membranous) in chRCC *vs.* RO.

Immunohistochemistry showing S100A1 nuclear expression

When nuclear expression of S100A1 was analysed, there was no significant difference between tumour and non-neoplastic tissue (*Figure 8*). Separately for ccRCC and RO (*Figures 8B,D*), there was higher expression in the tumours compared to non-neoplastic tissue, but the difference did not reach significance. However in chRCC, there was lower S100A1 nuclear expression in the tumour compared to non-cancer kidney (P=0.11); however this did not reach statistical significance (*Figure 8C*). There was higher expression of S100A1 in nuclear regions of RO in contrast to chRCC but this did not reach significance (P=0.06) (*Figures 8E,F*).

Discussion

Histopathological diagnosis of kidney tumour subtypes poses a significant diagnostic dilemma when the morphological characteristics of tumour subtypes overlap (10). Obviously, the distinction for RO from chRCC will dictate different management pathways as RO is benign while chRCC is a malignant subtype which, depending on the chRCC variants, will require further surveillance or surgery. Another important distinction is chRCC from ccRCC, as chRCC may have a favourable prognosis compared to ccRCC (11).

Traditionally, Hale colloidal iron staining has been used to distinguish chRCC from the other mimics. However, the reproducibility of Hale colloidal iron staining is technically-difficult, due to variations in pH, leading to difficulty in interpretation (12), and inconsistent reproducibility of results. Ultrastructurally, chRCC has numerous cytoplasmic microvesicles and RO, on the other hand, has abundant giant mitochondria (13), but electron microscopy facilities are not readily available, and this technique is not clinically practical in an era when cost and time must always be considered. Therefore utility of various immunohistochemical biomarkers remains the most readily accessible and efficient method of distinguishing RO and chRCC. Biomarkers CK7, Cav-1 and S100A1 were chosen following results from our

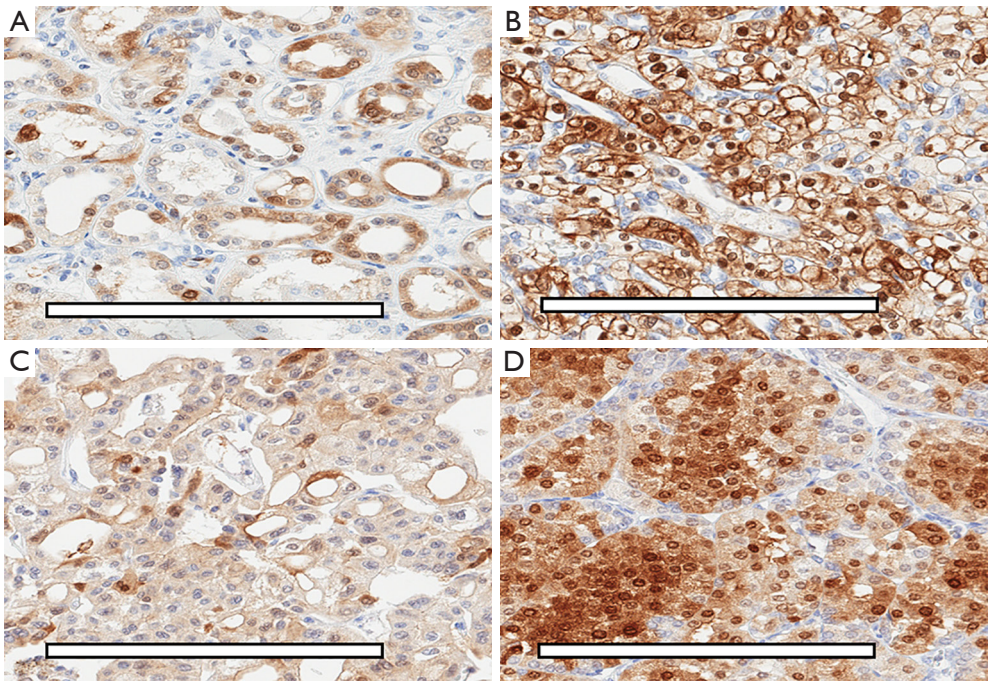

Figure 6 S100A1 immunostaining in non-neoplastic renal cortical tissue and renal tumour tissue. (A) Immunostaining of S100A1 in adjacent non-neoplastic renal cortical tissue showing mainly cytoplasmic staining; (B) in clear cell renal cell carcinoma (RCC), there was membranous and cytoplasmic S100A1 staining; (C) there was patchy cytoplasmic S100A1 staining in chromophobe RCC; (D) intense and diffuse cytoplasmic and nuclear staining of S100A1 in renal oncocytoma. Scale bar =200 µm.

recent meta-analysis that identified a panel of significant immunohistochemical biomarkers that can discriminate between chRCC and RO (2).

CK7

Cytokeratins are important markers of epithelial differentiation. They consist of at least 20 distinct molecules, the expression of which depends on cell type and differentiation status, making them useful in differential diagnosis of many epithelial tumours (4). As a result CK7 has been widely investigated as a biomarker in kidney neoplasms, including the distinction of chRCC from other mimicking kidney tumours (e.g., RO, and eosinophilic variants of chRCC). In the current study, CK7 immunostaining was seen in cytoplasm of non-neoplastic distal tubular cells. This is consistent with published reports where CK7 staining in non-neoplastic kidney was expressed in distal tubules and collecting ducts (14). There was minimal CK7 staining in ccRCC and RO in our study; with diffuse cytoplasmic and peripheral membranous enhancement in chRCC. This agrees with previous work, where in chRCC there was diffuse cytoplasmic staining with peripherally-enhanced expression while only weak patchy sporadic expression was reported in RO (15,16). In addition, CK7 expression was weak or absent in most of our ccRCC. The strong expression of chRCC compared with weak or absent expression in RO and ccRCC is consistent with previous published results (17-20). The exact reason behind these expression differences in these 3 subtypes of kidney tumours remains to be elucidated.

The strong and enhanced peripheral membranous immunostaining noted in the chRCC cases may reflect the peripheral distribution of intermediate filaments within the tumour cells. Abundant cytoplasmic microvesicles in chRCC may push the intermediate filaments aside in the peripheral area of the cytoplasm, because chRCC has more abundant cytoplasmic microvesicles (21). Overall expression of chRCC was highest amongst the three tumour subtypes and was significantly higher compared to RO. This differential immunohistochemistry result between positively-stained chRCC versus poorly-stained RO in this Australian cohort of patients provides further validation of other published results (9,11,16,22). However, there were also some authors who had results where CK7 expression was prominent on RO

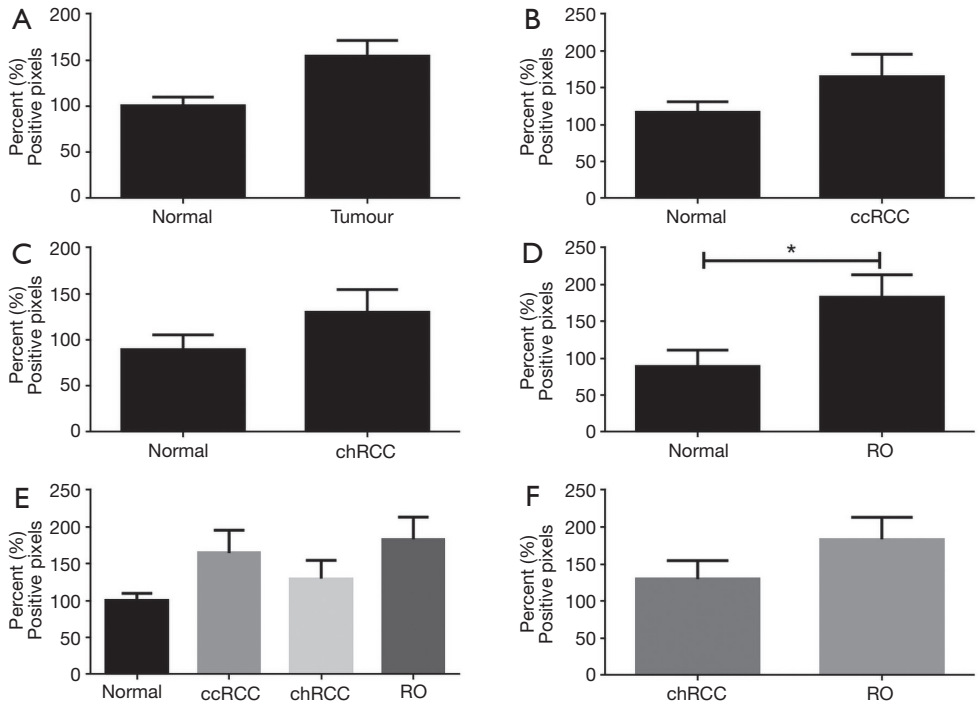

Figure 7 S100A1 expression in renal tumours and matched non-neoplastic renal tissue. (A) S100A1 expression in tumour *vs.* non-neoplastic kidney; (B) S100A1 expression in clear cell (cc) renal cell carcinoma (RCC) *vs.* non-neoplastic kidney; (C) S100A1 expression of chromophobe (ch) RCC *vs.* non-neoplastic kidney; (D) increased S100A1 expression in renal oncocytoma (RO) *vs.* non-neoplastic kidney (*, P=0.02); (E) expression of S100A1 across tumour subtypes; (F) expression of S100A1 in RO *vs.* chRCC (non-significant).

compared to chRCC (23,24). Small numbers of chRCC and RO used in the investigations may produce disparate results, difficult histological interpretation of immunohistochemistry and inaccurate initial diagnoses of the cases. Nevertheless, the CK7 immunohistochemistry study provided similar results as revealed by our meta-analysis, where CK7 has been identified as the most studied immunohistochemical biomarker in the differentiation between chRCC and RO (2). From this meta-analysis, we also recommended CK7 as part of a panel of immunohistochemical biomarkers than could be useful in differentiating chRCC from RO. Other authors have also recommended CK7 as part of their panel of immunohistochemical biomarkers for this purpose (9,25,26).

The association of CK7 with RCC tumourigenesis or progression needs further evaluation. One proposed mechanism includes matrix metalloproteinases (MMP). It is possible that the clinical behaviour and better prognosis of chRCC in contrast to other RCC could be related to the association of CK7 with absence of membrane type 1 MMP (MT1-MMP). MMPs are zinc-dependent endopeptidases, which are largely involved in tissue remodelling, degradation of the extracellular matrix and basal membranes leading to tumour invasion and progression (27). One study showed the absence of MT1-MMP in CK7-positive ccRCC, suggesting that any good prognosis of CK7-expressing ccRCC can be partially explained by absence of MT1-MMP expression (14). Further work should focus on pathophysiology responsible for the increased expression of CK7 in chRCC compared to minimal or patchy expression in RO as both tumours originate from intercalated cells of collecting duct, which also expresses CK7. One study proposed that most biomarkers that are expressed in the collecting duct system may show decreased expression or disappear in many RO because cell-to-cell interactions of the majority of RO decrease during tumorigenesis (28). In addition, the association of expression of CK7 in chRCC with cancer specific survival should also be investigated.

Caveolin-1

Caveolae are specialized lipid raft microdomains forming

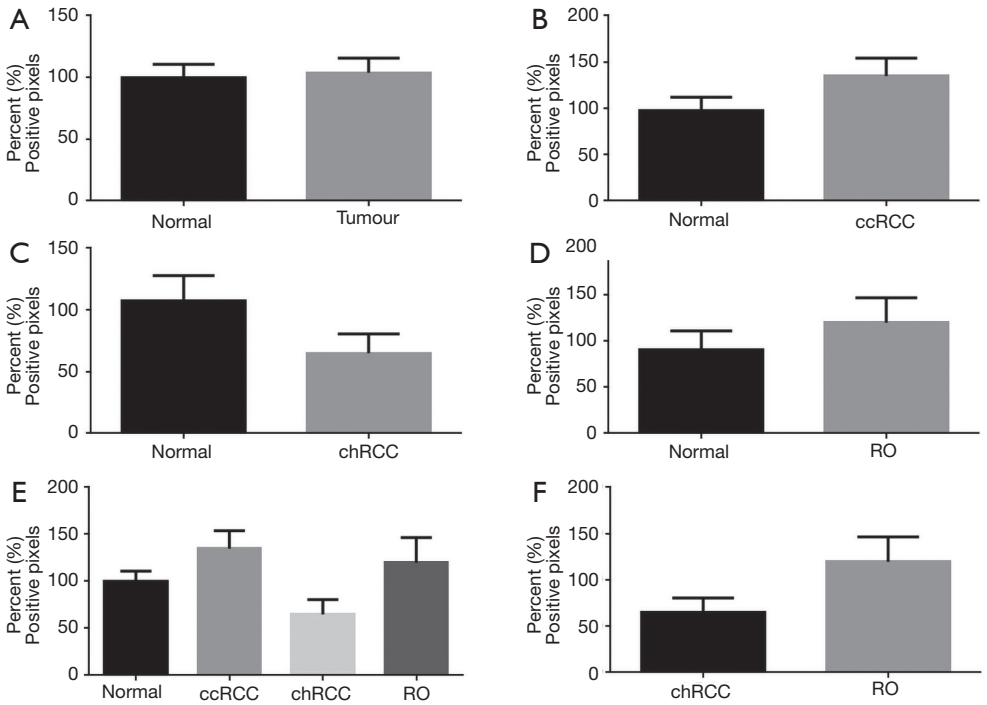

Figure 8 S100A1 nuclear expression in renal tumours and matched non-neoplastic renal tissue. (A) S100A1 expression in tumour *vs.* non-neoplastic kidney; (B) S100A1 expression in clear cell (cc) renal cell carcinoma (RCC) *vs.* non-neoplastic kidney; (C) S100A1 expression of chromophobe (ch) RCC *vs.* non-neoplastic kidney; (D) increased S100A1 expression in renal oncocytoma (RO) *vs.* non-neoplastic kidney; (E) expression of S100A1 across tumour subtypes; (F) expression of S100A1 in RO *vs.* chRCC (P=0.06).

50 to 100 nm flask-shaped vesicular invaginations of the plasma membrane, which serve as a scaffold for signalling molecules related to cell adhesion, growth and survival (29). Caveolins are functionally and structurally highly conserved, and they initiate caveolae formation from raft derived components. Cav-1 is involved in the regulation of numerous signalling cascades, including receptor and non-receptor tyrosine kinases such as epidermal growth factor, Neu and the Src family tyrosine kinases, protein kinase C, heterotrimeric G-protein α-subunits and endothelial nitric oxide synthase (30). Some studies have demonstrated that Cav-1 acts as a tumour suppressor protein, inhibiting the functional signalling activity of several proto-oncogenes and, consequently, disrupting the process of cellular transformation (4). Expression of Cav-1 has been studied in various types of tumours; and previous authors have published results in RCC (31-33).

From our study, there was minimal staining of Cav-1 noted in distal tubules and more pronounced staining of endothelial cells in non-neoplastic kidney tissue. This is reflective of previous studies where Cav-1 was localised to distal tubular cells, collecting ducts, parietal cells of Bowman's capsule, endothelial and smooth muscle cells (34). All three tumours (ccRCC, chRCC and RO) demonstrated significantly higher overall and membranous expression of Cav-1 compared to non-neoplastic kidney tissue. There was prominent membranous staining of Cav-1 in ccRCC. In chRCC, intense diffuse cytoplasmic staining with peripheral membranous enhancement and a distinctive perinuclear halo was noted; while in RO there was patchy cytoplasmic staining. Membranous expression of Cav-1 was highest in ccRCC followed by chRCC and RO. The staining patterns of the 3 tumours were similar to reports published by Tamaskar *et al.*, where ccRCC were noted to have predominantly membranous expression while chRCC and RO had cytoplasmic expression (35). Similarly Mete *et al.* also recorded a difference in staining patterns between chRCC (diffuse and peripheral cytoplasmic) and RO (diffuse cytoplasmic) (32). The observations by previous authors strengthen our findings of differences in staining patterns noted in our chRCC and RO. The differential immunohistochemistry staining pattern for Cav-1 between

the two entities will aid in the important differentiation of the two tumours.

Although increased overall and membranous expression of Cav-1 was noted in chRCC compared with RO, these were not statistically significant. Other published results have also shown that Cav-1 expression was higher in the majority of chRCC versus focal positivity in the minority of RO (33,36). However, one contrasting report had RO with increased cytoplasmic staining and lower expression in chRCC (31). Nonetheless, the different staining patterns may be beneficial in differentiation between chRCC and RO. The significance of Cav-1 over-expression in RCC has been linked to higher tumour grades, venous invasion, lymph node metastases, tumour progression and poorer prognosis (37). It is well known that ccRCC have a more aggressive malignant nature and therefore, as expected, the highest expression of Cav-1 was noted in ccRCC compared to chRCC (less aggressive but malignant) and benign RO. A recent meta-analysis reported the association of Cav-1 levels with cancer-specific survival in kidney cancers with a hazard ratio of 1.98 (38).

The mechanisms by which Cav-1 exerts its tumourigenic effect include enhancement of vascular endothelial growth factor (VEGF) secretion, thereby stimulating angiogenesis (39); and interaction with phospho-ERK-1/2 to promote tumour survival and growth (40). Also in RCC, Cav-1 may serve as a 'gatekeeper' for activation of the hypoxia-inducible factor (HIF) pathway. HIF is a downstream effector molecule of mammalian target of rapamycin (mTOR) that accumulates in RCC in response to the loss of function of the Von Hippel Lindau (VHL) gene and promotes angiogenesis, vascular invasion and chemoresistance (41). In summary, Cav-1 can be utilised as diagnostic tool, prognostic indicator and also a possible therapeutic target in RCC. Here we highlight the use of Cav-1 immunohistochemical differential staining patterns as an aid to distinguish chRCC from RO.

S100A1

S100A1 is a member of the S100 family, the largest subgroup of the EF-hand proteins (42). S100A1 has been reported to be involved in different biological activities such as transduction of intracellular calcium signalling, cytoskeleton-mediated interactions, as well as cell cycle progression and cell differentiation (43). Therefore it has been studied in a variety of tumours, including kidney cancers. From the present study, S100A1 immunostaining was noted in nuclei and cytoplasmic regions of proximal tubular cells and collecting ducts in adjacent non neoplastic kidney parenchyma. This is similar to previous published results (44). In ccRCC, strong S100A1 immunostaining in cytoplasmic and membranous regions of tumour cells was noted, while there was only patchy minimal cytoplasmic expression in chRCC and strong diffuse cytoplasmic and nuclear staining in RO. In comparing the recent studies examining immunohistochemistry expression of S100A1 in kidney neoplasms, ccRCC was found to have expression in 66–73% of cases and 67–94% of papillary RCC. The highest level of expression was identified in RO, with 92–93% of cases demonstrating reactivity with S100A1 compared to 0–6% of chRCC, which have been found to be negative (5,25,44). Recently, Kuroda *et al.* reported that immunohistochemical cytoplasmic expression of S100A1 was 100% of ROs compared to only 30% of chRCC (45).

The immunohistochemistry results of the present study were in agreement with the differential immunostaining of S100A1 in RO compared with chRCC. There was apparent higher overall and nuclear expression of S100A1 in RO over chRCC in our cohort, but this unfortunately did not reach statistical significance. This is perhaps related to the small RO sample size of 15 cases. Nevertheless, the majority of RO in the study expressed diffusely intense cytoplasmic and nuclear staining of S100A1 compared with minimal patchy cytoplasmic expression in chRCC, similar to other published reports. Therefore, S100A1 is another reproducible immunohistochemical biomarker from a panel of biomarkers that can differentiate RO from chRCC (2). Other authors have suggested a panel of CK7, S100A1 and claudin 8 (25), and the utility of cluster analysis of S100A1 and CK7 (46), which could discriminate the two entities. Conner *et al.* have reported the usefulness of S100A1 immunohistochemistry in fine needle aspirates and core needle biopsies that showed positivity in 80% of RO versus 8% in chRCC (47). This could provide a valuable distinction between the two entities in selective groups of patients with indeterminate small kidney masses.

Conclusions

This study of an Australian cohort of patients has validated some of the immunohistochemistry results of CK7, S100A1 and Cav-1 from previous studies: significantly higher CK7 expression in chRCC than in RO; higher expression of S100A1 in RO than in chRCC; and higher expression of Cav-1 with different staining patterns for chRCC

when compared to RO. The application of this panel of biomarkers may enhance the reliable characterization of these histologically difficult to separate kidney lesions.

Acknowledgments

We thank Mr Clay Winterford (QIMR Berghofer Medical Research Institute, Herston, Australia) for his assistance with immunohistochemical staining of S100A1.

Footnote

Conflicts of Interest: Author's Note: This manuscript was adapted from material included in Dr. Keng Lim Ng's PhD Thesis.

Ethical Statement: Use of stored paraffin blocks in this study was approved by the ethics committee of Aquesta Pathology (protocol 14/02). Informed consent was taken from all the patients.

References

1. Gandaglia G, Ravi P, Abdollah F, et al. Contemporary incidence and mortality rates of kidney cancer in the United States. Can Urol Assoc J 2014;8:247-52.
2. Ng KL, Morais C, Bernard A, et al. A systematic review and meta-analysis of immunohistochemical biomarkers that differentiate chromophobe renal cell carcinoma from renal oncocytoma. J Clin Pathol 2016;69:661-71.
3. Skinnider BF, Folpe AL, Hennigar RA, et al. Distribution of cytokeratins and vimentin in adult renal neoplasms and normal renal tissue: potential utility of a cytokeratin antibody panel in the differential diagnosis of renal tumors. Am J Surg Pathol 2005;29:747-54.
4. Cohen AW, Hnasko R, Schubert W, Lisanti MP. Role of caveolae and caveolins in health and disease. Physiol Rev 2004;84:1341-79.
5. Teratani T, Watanabe T, Kuwahara F, et al. Induced transcriptional expression of calcium-binding protein S100A1 and S100A10 genes in human renal cell carcinoma. Cancer Lett 2002;175:71-7.
6. Li G, Barthelemy A, Feng G, et al. S100A1: a powerful marker to differentiate chromophobe renal cell carcinoma from renal oncocytoma. Histopathology 2007;50:642-7.
7. Kawaguchi S, Fernandes KA, Finelli A, et al. Most renal oncocytomas appear to grow: observations of tumor kinetics with active surveillance. J Urol 2011;186:1218-22.
8. Delahunt B, Srigley JR, Egevad L, et al. International Society of Urological Pathology grading and other prognostic factors for renal neoplasia. Eur Urol 2014;66:795-8.
9. Duchene DA, Lotan Y, Cadeddu JA, et al. Histopathology of surgically managed renal tumors: analysis of a contemporary series. Urology 2003;62:827-30.
10. Liu L, Qian J, Singh H, et al. Immunohistochemical analysis of chromophobe renal cell carcinoma, renal oncocytoma, and clear cell carcinoma: an optimal and practical panel for differential diagnosis. Arch Pathol Lab Med 2007;131:1290-7.
11. Srigley JR, Hutter RV, Gelb AB, et al. Renal cell carcinoma: current prognostic factors. Union Internationale Contre le Cancer (UICC) and the American Joint Committee on Cancer (AJCC). Cancer 1997;80:994-6.
12. Leroy X, Moukassa D, Copin MC, et al. Utility of cytokeratin 7 for distinguishing chromophobe renal cell carcinoma from renal oncocytoma. Eur Urol 2000;37:484-7.
13. Cochand-Priollet B, Molinie V, Bougaran J, et al. Renal chromophobe cell carcinoma and oncocytoma. A comparative morphologic, histochemical, and immunohistochemical study of 124 cases. Arch Pathol Lab Med 1997;121:1081-6.
14. Mertz KD, Demichelis F, Sboner A, et al. Association of cytokeratin 7 and 19 expression with genomic stability and favorable prognosis in clear cell renal cell cancer. Int J Cancer 2008;123:569-76.
15. Bing Z, Lal P, Lu S, et al. Role of carbonic anhydrase IX, alpha-methylacyl coenzyme a racemase, cytokeratin 7, and galectin-3 in the evaluation of renal neoplasms: a tissue microarray immunohistochemical study. Ann Diagn Pathol 2013;17:58-62.
16. Mathers ME, Pollock Am, Marsh C, et al. Cytokeratin 7: a useful adjunct in the diagnosis of chromophobe renal cell carcinoma. Histopathology 2002;40:563-7.
17. Yasir S, Herrera L, Gomez-Fernandez C, et al. CD10+ and CK7/RON- immunophenotype distinguishes renal cell carcinoma, conventional type with eosinophilic morphology from its mimickers. Appl Immunohistochem Mol Morphol 2012;20:454-61.
18. Mazal PR, Exner M, Haitel A, et al. Expression of kidney-specific cadherin distinguishes chromophobe renal cell carcinoma from renal oncocytoma. Hum Pathol 2005;36:22-8.
19. Kuroda N, Toi M, Yanamoto M, et al.

Immunohistochemical identification of intracytoplasmic lumens by cytokeratin typing may differentiate renal oncocytomas from chromophobe renal cell carcinomas. Histol Histopathol 2004;19:23-8.
20. Geramizadeh B, Ravanshad M, Rahsaz M. Useful markers for differential diagnosis of oncocytoma, chromophobe renal cell carcinoma and conventional renal cell carcinoma. Indian J Pathol Microbiol 2008;51:167-71.
21. Latham B, Dickersin GR, Oliva E. Subtypes of chromophobe cell renal carcinoma: an ultrastructural and histochemical study of 13 cases. Am J Surg Pathol 1999;23:530-5.
22. Adley BP, Papavero V, Sugimura J, et al. Diagnostic value of cytokeratin 7 and parvalbumin in differentiating chromophobe renal cell carcinoma from renal oncocytoma. Anal Quant Cytol Histol 2006;28:228-36.
23. Taki A, Nakatani T, Misugi K, et al. Chromophobe renal cell carcinoma: an immunohistochemical study of 21 Japanese cases. Mod Pathol 1999;12:310-7.
24. Wu SL, Kothari P, Wheeler TM, et al. Cytokeratins 7 and 20 immunoreactivity in chromophobe renal cell carcinomas and renal oncocytomas. Mod Pathol 2002;15:712-7.
25. Kim SS, Choi YD, Jin XM, et al. Immunohistochemical stain for cytokeratin 7, S100A1 and claudin 8 is valuable in differential diagnosis of chromophobe renal cell carcinoma from renal oncocytoma. Histopathology 2009;54:633-5.
26. Memeo L, Jhang J, Assaad AM, et al. Immunohistochemical analysis for cytokeratin 7, KIT, and PAX2: value in the differential diagnosis of chromophobe cell carcinoma. Am J Clin Pathol 2007;127:225-9.
27. Nagase H, Woessner JF Jr. Matrix metalloproteinases. J Biol Chem 1999;274:21491-4.
28. Ohe C, Kuroda N, Takasu K, et al. Utility of immunohistochemical analysis of KAI1, epithelial-specific antigen, and epithelial-related antigen for distinction of chromophobe renal cell carcinoma, an eosinophilic variant from renal oncocytoma. Med Mol Morphol 2012;45:98-104.
29. Anderson RG. The caveolae membrane system. Annu Rev Biochem 1998;67:199-225.
30. Okamoto T, Schlegel A, Scherer PE, Lisani MP. Caveolins, a family of scaffolding proteins for organizing "preassembled signaling complexes" at the plasma membrane. J Biol Chem 1998;273:5419-22.
31. Carrion R, Morgan BE, Tannenbaum M, et al. Caveolin expression in adult renal tumors. Urol Oncol 2003;21:191-6.
32. Mete O, Kilicaslan I, Gulloglu MG, Uysal V. Can renal oncocytoma be differentiated from its renal mimics? The utility of anti-mitochondrial, caveolin 1, CD63 and cytokeratin 14 antibodies in the differential diagnosis. Virchows Arch 2005;447:938-46.
33. Garcia E, Li M. Caveolin-1 immunohistochemical analysis in differentiating chromophobe renal cell carcinoma from renal oncocytoma. Am J Clin Pathol 2006;125:392-8.
34. Breton S, Lisanti MP, Tyszkowski R, et al. Basolateral distribution of caveolin-1 in the kidney. Absence from H+-atpase-coated endocytic vesicles in intercalated cells. J Histochem Cytochem 1998;46:205-14.
35. Tamaskar I, Choueiri TK, Sercia L, et al. Differential expression of caveolin-1 in renal neoplasms. Cancer 2007;110:776-82.
36. Lee HW, Lee EH, Lee CH, et al. Diagnostic utility of Caveolin-1 and MOC-31 in distinguishing chromophobe renal cell carcinoma from renal oncocytoma. Korean J Urol 2011;52:96-103.
37. Horiguchi A, Asano T, Asakuma J, et al. Impact of caveolin-1 expression on clinicopathological parameters in renal cell carcinoma. J Urol 2004;172:718-22.
38. Liu JM, Cheng SH, Liu XX, et al. Prognostic value of caveolin-1 in genitourinary cancer: a meta-analysis. Int J Clin Exp Med 2015;8:20760-8.
39. Li L, Ren C, Yang G, et al. Caveolin-1 promotes autoregulatory, Akt-mediated induction of cancer-promoting growth factors in prostate cancer cells. Mol Cancer Res 2009;7:1781-91.
40. Campbell L, Al-Jayyoussi G, Gutteridge R, et al. Caveolin-1 in renal cell carcinoma promotes tumour cell invasion, and in co-operation with pERK predicts metastases in patients with clinically confined disease. J Transl Med 2013;11:255.
41. Patel PH, Chadalavada RS, Chaganti RS, et al. Targeting von Hippel-Lindau pathway in renal cell carcinoma. Clin Cancer Res 2006;12:7215-20.
42. Schäfer BW, Heizmann CW. The S100 family of EF-hand calcium-binding proteins: functions and pathology. Trends Biochem Sci 1996;21:134-40.
43. Li G, Gentil-Perret A, Lambert C, et al. S100A1 and KIT gene expressions in common subtypes of renal tumours. Eur J Surg Oncol 2005;31:299-303.
44. Rocca PC, Brunelli M, Gobbo S, et al. Diagnostic utility of S100A1 expression in renal cell neoplasms: an immunohistochemical and quantitative RT-PCR study. Mod Pathol 2007;20:722-8.
45. Kuroda N, Kanomata N, Tamaguchi T, et al.

Immunohistochemical application of S100A1 in renal oncocytoma, oncocytic papillary renal cell carcinoma, and two variants of chromophobe renal cell carcinoma. Med Mol Morphol 2011;44:111-5.
46. Carvalho JC, Wasco MJ, Kunju LP, et al. Cluster analysis of immunohistochemical profiles delineates CK7, vimentin, S100A1 and C-kit (CD117) as an optimal panel in the differential diagnosis of renal oncocytoma from its mimics. Histopathology 2011;58:169-79.
47. Conner JR, Hirsch MS, Jo VY. HNF1beta and S100A1 are useful biomarkers for distinguishing renal oncocytoma and chromophobe renal cell carcinoma in FNA and core needle biopsies. Cancer Cytopathol 2015;123:298-305.

Cite this article as: Ng KL, Ellis RJ, Samaratunga H, Morais C, Gobe GC, Wood ST. Utility of cytokeratin 7, S100A1 and caveolin-1 as immunohistochemical biomarkers to differentiate chromophobe renal cell carcinoma from renal oncocytoma. Transl Androl Urol 2019;8(Suppl 2):S123-S137. doi: 10.21037/tau.2018.11.02

